Automated Date Palm Detection and Geometric Analysis Using UAV Imagery and Deep Learning

Mustafa Milad Aburas1, Maher M Aburas2*Emad Salim Altaeb3

[1.] Higher Institute of Science and Technology Al-Shumookh, Tripoli, Libya

[2.] Higher Institute for Engineering Technologies Al-Majori, Benghazi, Libya

[3.] Higher Institute for Engineering Technologies Alqwarsha, Benghazi, Libya

*Corresponding Author: maheraburas@tve.gov.ly

ABSTRACT

Accurate inventory and structural assessment of date palm trees are essential for effective agricultural management in semi-arid environments. Conventional field-based surveys are labor-intensive, time-consuming, and often impractical for large plantation areas. This study proposes an automated framework that integrates high-resolution unmanned aerial vehicle (UAV) imagery, deep learning, and geographic information systems (GIS) for the detection, counting, and geometric analysis of date palm trees. A low-altitude UAV survey was conducted over a 3.66-ha date palm farm in Al-Kararim, Misrata, Libya, acquiring 466 aerial images with a ground sampling distance of 1.77 cm. Photogrammetric processing produced high-accuracy orthomosaics and digital elevation models, achieving a total root mean square error of 5.06 cm. A YOLO-based deep learning model was trained on annotated UAV imagery and achieved a mean average precision (mAP@50) of 93.0% with a recall of 95.1%. The model successfully detected 310 out of 360 palm trees (86%), with undetected cases mainly corresponding to very young seedlings with limited canopy development. Geometric parameters, including canopy diameter and tree height, were extracted by integrating detection outputs with elevation data, and unique spatial identifiers were assigned to each palm. All results were compiled into a geospatial database within ArcGIS Pro, enabling advanced spatial and statistical analyses. The proposed framework demonstrates strong potential for scalable and data-driven precision agriculture applications in arid and semi-arid regions.

Received: 16-02-2026 - Accepted: 24-02-2026 - Published: 02-03-2026

Keywords. : Unmanned aerial vehicle (UAV); Date palm trees; Deep learning; YOLO; Automated detection; Geometric analysis; Geographic information systems (GIS)

1. Introduction

Date palm cultivation represents a cornerstone of agricultural production in arid and semi-arid regions, where it plays a vital role in food security, rural livelihoods, and ecological stability (Chao and Krueger 2007, El Hadrami and Al-Khayri 2012). Owing to its high tolerance to drought, salinity, and extreme temperatures, date palm is

widely cultivated across North Africa and the Middle East, forming a key component of oasis-based and irrigated farming systems (Zaid and Arias-Jimenez 2002). Effective management of date palm plantations requires accurate and up-to-date information on tree distribution, density, and structural characteristics, as these parameters directly influence irrigation planning, yield estimation, disease monitoring, and long-term sustainability (Zaid 2024). However, the spatial heterogeneity and large extent of many date palm farms pose significant challenges for consistent monitoring using conventional approaches, particularly in regions experiencing increasing pressure on water and land resources. Consequently, the adoption of advanced geospatial technologies has become essential to support precision agriculture and data-driven management of date palm agroecosystems.

Traditional approaches for inventorying and monitoring date palm plantations rely primarily on field-based surveys and manual measurements, which are often labor-intensive, time-consuming, and costly, particularly for large or densely planted farms (Laliberte and Rango 2011, Rasmussen, Ntakos et al. 2016). These methods are further constrained by limited spatial coverage and are prone to human error, resulting in inconsistencies in tree counts and structural measurements. In arid and semi-arid regions, harsh environmental conditions and restricted accessibility can significantly reduce the frequency and reliability of field surveys (Weinstein, Marconi et al. 2019). Moreover, conventional techniques lack the capacity to provide spatially explicit and temporally consistent data required for precision agriculture, such as detailed canopy geometry and height variability at the individual tree level. As a result, plantation managers often depend on outdated or incomplete information, which limits their ability to optimize irrigation, assess tree health, and implement timely management interventions (Zhang and Kovacs 2012). These limitations highlight the urgent need for efficient, scalable, and automated monitoring solutions capable of delivering accurate and repeatable measurements across entire agricultural landscapes.

Recent advances in unmanned aerial vehicle (UAV) technology and photogrammetric processing have significantly enhanced the capacity to acquire high-resolution spatial data for agricultural monitoring. UAV-based imagery enables the generation of detailed orthomosaics and digital elevation models that support precise mapping of vegetation structure at the individual tree level (Laliberte and Rango 2011, Torres-Sánchez, López-Granados et al. 2015). In parallel, the rapid development of deep learning algorithms, particularly convolutional neural networks (CNNs), has transformed object detection and classification tasks in remote sensing applications. Models such as You Only Look Once (YOLO) have demonstrated high efficiency and accuracy in detecting individual trees and crops from high-resolution UAV imagery (Li, Fu et al. 2016, Redmon, Divvala et al. 2016). These approaches have been successfully applied to a range of agricultural contexts, including orchard tree detection, crop counting, and canopy characterization (Ampatzidis and Partel 2019, Osco, Junior et al. 2021). By combining UAV photogrammetry with deep learning-based object detection, recent studies have shown strong potential for automating agricultural inventories and reducing reliance on labor-

intensive field surveys. Nevertheless, many existing applications focus primarily on detection accuracy, with limited integration of geometric measurements and spatial database management within a unified geospatial framework.

Despite the growing body of research on UAV-based mapping and deep learning–driven detection of agricultural trees, several limitations remain in existing studies. Many approaches focus primarily on object detection or counting accuracy, without extending the analysis to include detailed geometric parameters such as canopy dimensions and tree height at the individual tree level (Li, Fu et al. 2016, Osco, Junior et al. 2021). Furthermore, limited attention has been given to integrating detection results into structured geospatial databases that enable spatial querying, statistical analysis, and long-term monitoring within a geographic information system (GIS) environment (Ampatzidis and Partel 2019). In the context of date palm plantations, few studies have explored end-to-end frameworks that combine high-resolution photogrammetric products, deep learning–based detection, geometric analysis, and spatial data management in a single workflow. Additionally, challenges related to detecting young or sparsely developed palms remain underexplored, particularly in arid and semi-arid environments where background soil reflectance can significantly affect detection performance (Weinstein, Marconi et al. 2019). These gaps highlight the need for a comprehensive and scalable methodology that not only automates detection but also supports detailed structural assessment and geospatial decision-making for plantation management.

In response to the identified research gaps, this study aims to develop and evaluate an integrated framework for automated date palm detection and geometric analysis using high-resolution UAV imagery and deep learning techniques. The proposed methodology combines low-altitude UAV photogrammetry, a YOLO-based object detection model, and GIS-based spatial data management to produce an accurate and scalable inventory of date palm trees at the individual level. The framework was implemented and validated using a case study in Al-Kararim, Misrata, Libya, representing a typical semi-arid agricultural environment. In addition to automated detection and counting, the approach enables the extraction of key geometric parameters, including canopy diameter and tree height, through the integration of detection outputs with digital elevation models. Furthermore, all results are organized within a geospatial database to support spatial analysis, visualization, and decision-making for plantation management. By delivering an end-to-end, geospatially enabled workflow, this study contributes a practical and transferable solution for precision agriculture applications in arid and semi-arid regions, while also highlighting the limitations and opportunities associated with detecting young date palm seedlings using UAV-based deep learning approaches.

2. Methodology

2.1 Study Area

The study was conducted in the Al-Kararim area, located in the city of Misrata, northwestern Libya. The selected study site consists of a date palm plantation covering an area of approximately 3.66 ha and represents a typical

agricultural setting in a semi-arid environment. The plantation is characterized by relatively regular planting patterns and mixed growth stages of date palm trees, including mature palms and young seedlings. These characteristics make the site suitable for evaluating the performance of UAV-based photogrammetry and deep learning techniques for automated detection and geometric analysis at the individual tree level. The choice of this study area was motivated by its agricultural relevance, accessibility for UAV operations, and its representativeness of date palm farming systems commonly found in arid and semi-arid regions.

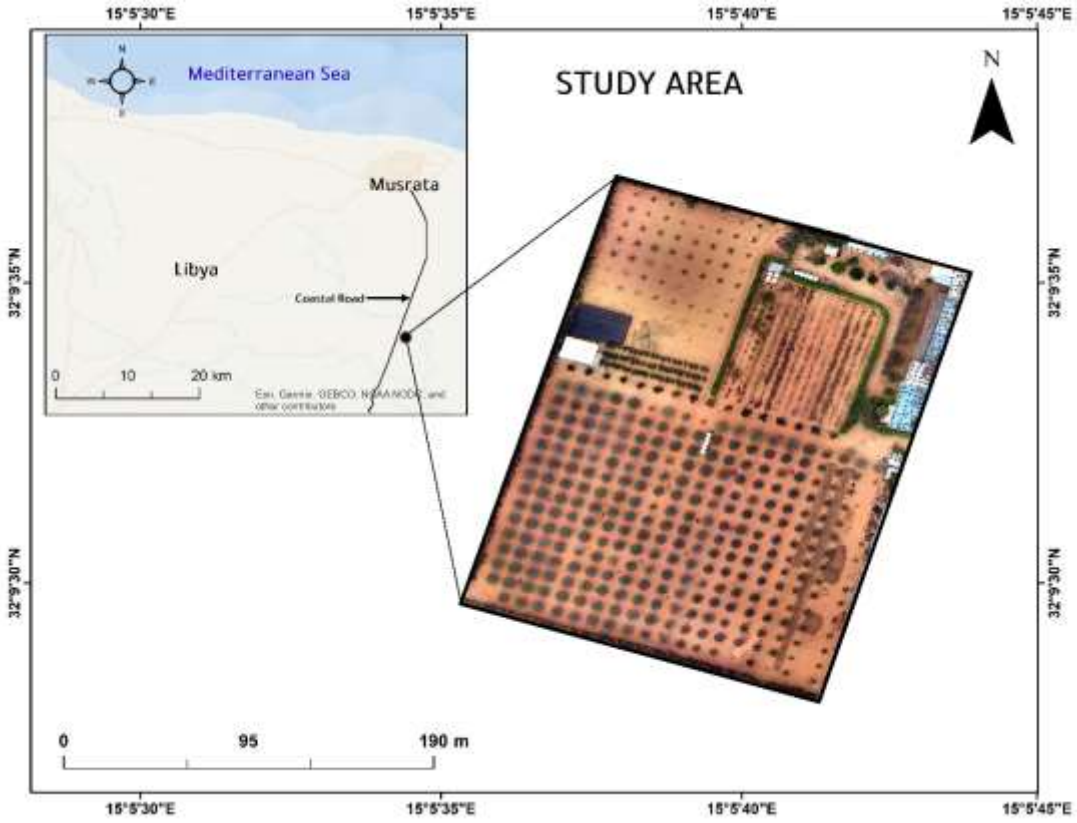

Figure 1. Study area

2.2 UAV Data Acquisition

A low-altitude aerial survey was conducted over the study area using a DJI Matrice 30T unmanned aerial vehicle to acquire high-resolution imagery for photogrammetric processing and automated analysis. The DJI Matrice 30T platform integrates advanced navigation and imaging capabilities suitable for precise geospatial data collection (Figure 1). The flight mission was planned to ensure complete coverage of the plantation with sufficient image overlap, enabling accurate three-dimensional reconstruction (Westoby et al., 2012). A total of 466 aerial images were acquired, achieving a ground sampling distance of 1.77 cm.

Figure 2. Overview of the DJI Matrice 301 nsing technologies.

To improve the geometric accuracy of the photogrammetric outputs, five ground control points (GCPs) and one reference point were established and surveyed within the study area. The GCPs were strategically distributed across the plantation to provide robust spatial control during image alignment and georeferencing (James et al., 2017). Each control point was recorded using geographic coordinates (longitude and latitude) and orthometric height, providing three-dimensional ground reference data. The spatial deployment of the GCPs during fieldwork is illustrated in Figure 3, while their geographic coordinates and elevation values are presented in Table 1. The UAV imagery and GCP measurements constituted the primary inputs for subsequent photogrammetric processing and deep learning-based analysis.

Figure 3. GCPs used for georeferencing during UAV field survey.

Table 1. Ground control points (GCPs) used in the UAV survey

P.ID	Longitude	Latitude	Orthometric Height (m)
1	15.09498339	32.15896089	5.763
2	15.09445550	32.15998133	4.855
3	15.09412084	32.15907619	5.510
4	15.09387145	32.15814693	5.228
5	15.09341328	32.15902252	5.405
Ref0	15.09493167	32.15894398	5.530

2.3 Data Processing

The UAV image block was processed using Agisoft Metashape Professional (v2.2.0 build 19757) to generate georeferenced photogrammetric products for subsequent analysis. Image alignment was performed for 466 images under High accuracy settings, producing 791,016 tie points and 3,338,483 projections, as summarized in Table 2. The overall alignment quality was verified by a mean reprojection error of approximately 1.29 pixels (RMS reprojection error of 1.29357 pixels), indicating a stable and well-constrained bundle adjustment (Table 2). The spatial geometry of the image network, including camera locations and image overlap, is presented in Figure 3, demonstrating consistent coverage across the study area.

Table 2. Summary of photogrammetric processing statistics and accuracy indicators.

Metric	Value
Number of images	466
Flying altitude	51.4 m
Ground resolution (GSD)	1.77 cm/pixel
Tie points	791,016
Projections	3,338,483
Reprojection error	~1.29 pixels
Total GCP RMSE	5.07 cm
Horizontal (XY) RMSE	4.95 cm
Vertical (Z) RMSE	1.07 cm

Ground control points (GCPs) were incorporated to enhance the georeferencing accuracy of the photogrammetric model. The positional accuracy was assessed using the root mean square error (RMSE), which is widely applied in photogrammetric and remote sensing studies to quantify spatial error (James et al., 2017; Westoby et al., 2012). The RMSE was computed as:

$$RMSE = \sqrt{\frac{1}{n}\sum_{i=1}^{n}(X_i - X_i^{ref})^2} \quad (1)$$

where Xi represents the estimated coordinate, Xiref is the corresponding reference coordinate obtained from field-surveyed GCPs, and n is the number of control points.

To distinguish between horizontal and vertical accuracy components, the RMSE was further expressed as:

$$RMSE_{XY} = \sqrt{\frac{1}{n}\sum_{i=1}^{n}\left[(X_i - X_i^{ref})^2 + (Y_i - Y_i^{ref})\right]} \quad (2)$$

$$RMSE_Z = \sqrt{\frac{1}{n}\sum_{i=1}^{n}(Z_i - Z_i^{ref}))^2} \quad (3)$$

The resulting accuracy assessment yielded a total RMSE of 5.07 cm, with horizontal RMSE (XY) = 4.95 cm and vertical RMSE (Z) = 1.07 cm, demonstrating high geometric fidelity of the reconstructed model (Table 2).

Following successful alignment and optimization, the georeferenced model was used to generate a high-resolution orthomosaic and digital elevation model (DEM). These products constituted the primary spatial inputs for deep learning-based detection and subsequent geometric analysis of individual date palm trees. Both a Digital Surface Model (DSM) and a Digital Terrain Model (DTM) were generated from the dense point cloud in Agisoft Metashape. Ground points were classified using the built-in ground filtering algorithm (progressive morphological filtering), with default parameterization adapted to low-relief agricultural terrain. The DTM was interpolated from classified ground points, while the DSM represented the full surface including vegetation canopy. A normalized Digital Surface Model (nDSM) was subsequently computed (nDSM = DSM – DTM) to derive tree height values. Individual palm height was extracted by calculating the maximum canopy elevation within each detected crown relative to the corresponding ground surface derived from the DTM.

2.4 Automated Date Palm Detection Using Deep Learning

Following the generation of georeferenced photogrammetric products, automated date palm detection was conducted using a deep learning–based object detection framework. The orthomosaic produced from the UAV imagery was used as the primary input dataset for model training and inference. A You Only Look Once (YOLO) architecture was adopted due to its high detection accuracy and real-time performance in aerial image analysis (Redmon et al., 2016).

Training data preparation involved manual annotation of date palm crowns using bounding boxes, followed by dataset augmentation to improve model generalization under varying illumination and canopy conditions. The annotated dataset was divided into training, validation, and testing subsets. Model training and inference were performed using Python within a Visual Studio Code environment (Figure 4).

The trained model was applied to the full orthomosaic to automatically detect individual date palm trees and generate spatial outputs containing bounding box coordinates and confidence scores. Detection performance was evaluated using standard metrics, including precision, recall, and mean Average Precision at an Intersection over Union threshold of 0.5 (mAP@50), ensuring reliable identification of palm trees across the study area.

The resulting detections formed the basis for subsequent geometric analysis and spatial integration within the GIS environment.

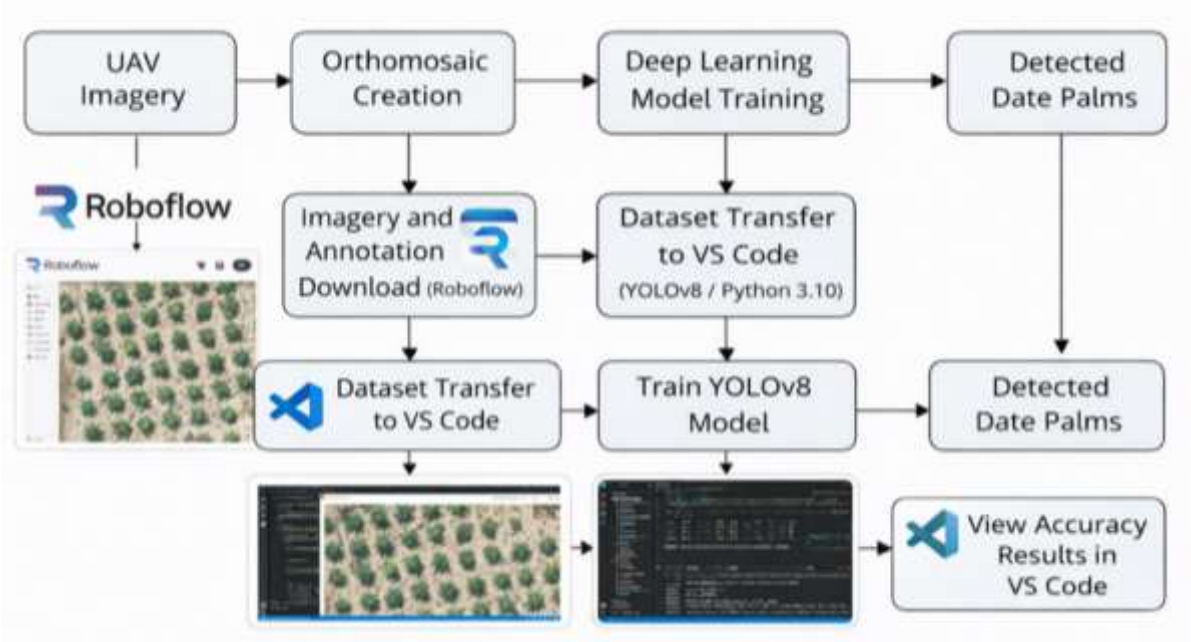

Figure 4. Flowchart of Date Palm Detection Using Deep Learning.

2.5 Geometric Analysis of Date Palm Trees

Following automated detection, geometric characteristics of individual date palm trees were extracted by integrating the deep learning outputs with elevation data derived from the photogrammetric products. The bounding boxes generated by the YOLOv8 model were converted into spatial features and linked to the digital elevation model (DEM) to enable per-tree measurements. Tree height was estimated by calculating the elevation difference between the canopy surface and the ground level, while canopy size was derived from the spatial extent of detected crowns in the orthomosaic. Each detected palm was assigned a unique spatial identifier to avoid duplication and to support individual-based analysis. The resulting geometric parameters provided quantitative descriptors of tree structure and formed the basis for subsequent spatial analysis and database integration (Figure 5) (Wallace et al., 2016).

The performance and accuracy of the deep learning model were evaluated within the Visual Studio Code (VS Code) environment during training and validation. Standard object detection metrics, including precision, recall, and mean Average Precision at an Intersection over Union threshold of 0.5 (mAP@50), were automatically computed by the YOLOv8 framework and monitored through training logs and evaluation outputs. These metrics provided quantitative evidence of the reliability of the detection results and ensured that the extracted geometric parameters were derived from accurately identified palm trees. The validated detection outputs subsequently served as the basis for spatial analysis and integration within the GIS environment.

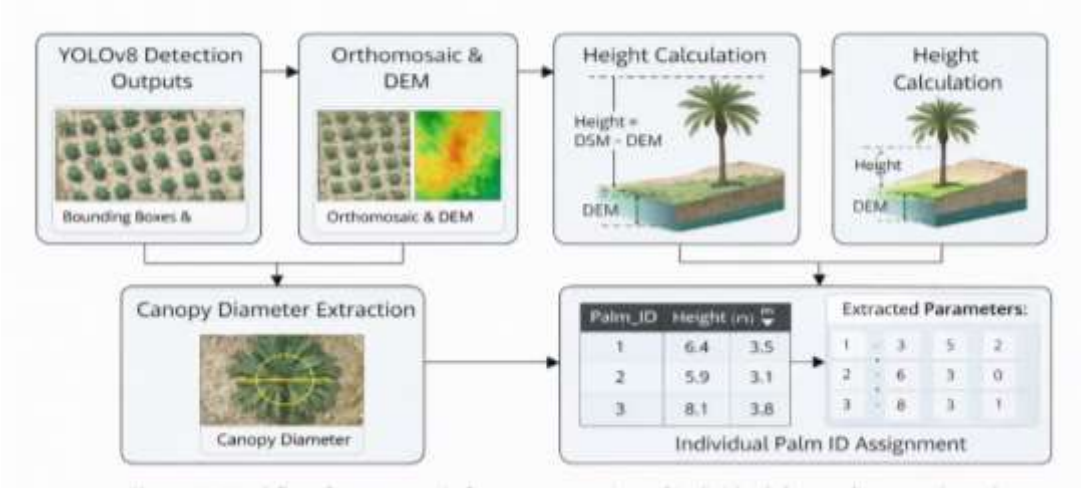

Figure 5. Workflow for geometric feature extraction and individual palm identification, showing the integration of YOLOv8 detection outputs with photogrammetric elevation data to derive tree height and canopy diameter, followed by the assignment of a unique Palm_ID and a schematic representation of the extracted attribute vectors for each detected date palm.

The 4. Results and Discussion

4.1 Automated Detection and Inventory of Date Palm Trees

The proposed deep learning framework demonstrated strong performance in automated date palm detection across the study area. The YOLOv8 model successfully detected 310 individual palms out of a total of 360 field-verified trees, corresponding to an overall detection rate of approximately 86%. The spatial distribution of the detected palms, including bounding boxes and assigned Palm_ID labels, is illustrated in Figure 6, where detections are overlaid on the high-resolution UAV orthomosaic.

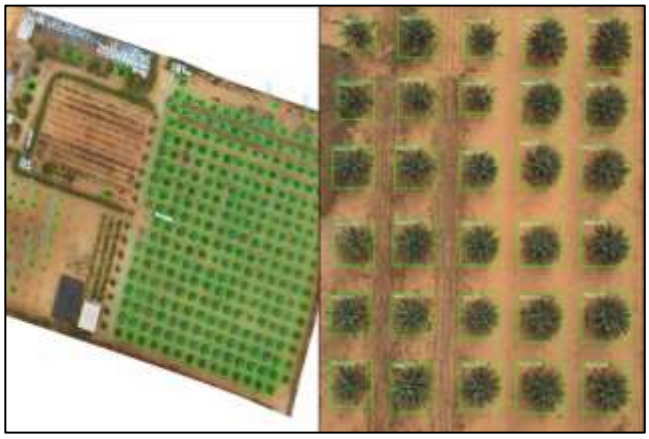

Figure 6. Automated detection results showing YOLOv8 bounding boxes and Palm_ID assignments overlaid on the UAV-derived orthomosaic.

The detection outputs show accurate localization of mature and structurally developed palms across the southern and central plantation blocks. The high ground sampling distance (1.77 cm) derived from the UAV survey enabled precise crown delineation and spatial positioning, supporting reliable object-level detection. The integration of detection results within the GIS environment further confirmed spatial consistency with the actual planting rows and farm layout.

Despite the high overall performance, 50 palms were not detected. Detailed inspection indicates that these omissions were almost exclusively associated with very young seedlings, characterized by small canopy diameters and limited spectral contrast relative to the surrounding soil background. This limitation is consistent with known challenges in small-object detection within high-resolution aerial imagery, where insufficient pixel representation reduces model confidence (Lin et al., 2014).

The quantitative performance metrics obtained during model evaluation in the VS Code environment further validate the robustness of the detection stage. The trained model achieved a mean Average Precision at IoU 0.5 (mAP@50) of 93.0% and a recall of 95.1%, indicating high detection reliability for palms with clearly defined structural features. The strong recall value confirms that the majority of mature palms were successfully identified, while missed detections were concentrated within early growth stages.

The reported mAP@50 (93.0%) and recall (95.1%) were calculated during model validation using the testing subset under an IoU threshold of 0.5 within the YOLO framework. These metrics reflect bounding-box detection performance at the object level under controlled validation conditions.

In contrast, the site-level detection rate of 86% was derived from full-orthomosaic inference and subsequent spatial matching with 360 field-verified trees. A spatial matching tolerance (IoU ≥ 0.5 and centroid proximity threshold) was applied to associate predicted boxes with ground-truth palm locations. The reduced detection rate at site scale was primarily influenced by (1) very small seedlings below the effective pixel representation threshold, (2) conservative confidence thresholding to minimize false positives, and (3) strict spatial matching criteria during post-processing.

False positives were minimal and were excluded during GIS-based verification, which did not substantially affect the recall metric but influenced final inventory statistics. A confusion matrix derived from orthomosaic-level evaluation will be included to improve transparency and explicitly report true positives, false negatives, and false positives.

From an operational perspective, the achieved detection accuracy is sufficient to support plantation inventory, spatial planning, and yield monitoring applications. However, improving sensitivity toward early-stage palms may require targeted augmentation strategies, increased training samples of seedlings, or integration of additional spectral information such as thermal or multispectral indices.

4.2 Geometric Analysis of Palm Structural Attributes

4.2.1 Crown Diameter Distribution

The spatial distribution of crown diameter across the study area is presented in Figure 7. The extracted crown diameters reveal a clear structural gradient within the plantation. Larger crowns are predominantly concentrated in the central and southern blocks, corresponding to mature and fully developed palms. In contrast, smaller crown diameters are observed in peripheral and northern sections, representing newly planted or early-growth palms.

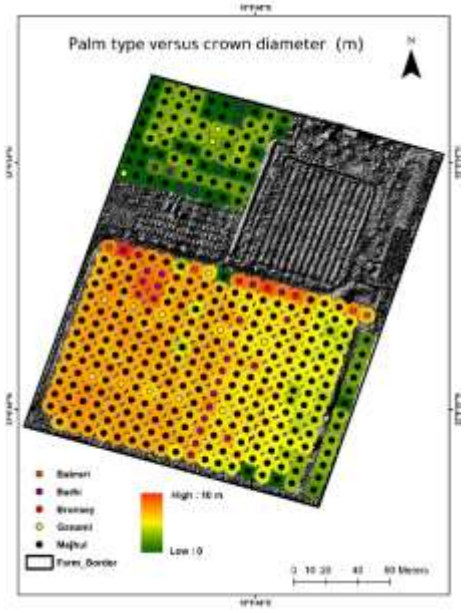

Figure 7. Spatial distribution of palm crown diameter (m) across the study area.

The spatial continuity of crown size reflects organized plantation design and phased agricultural development. The gradual transition in crown diameter across plantation zones indicates controlled management practices rather than random growth variability. Crown diameter therefore serves as a reliable horizontal structural indicator of palm maturity and productivity potential.

4.2.2 Tree Height Distribution

The spatial variation of tree height derived from the photogrammetric Digital Elevation Model (DEM) is illustrated in Figure 8. Extracted heights reached approximately 9.5 m, corresponding to mature productive palms. Taller palms are spatially concentrated in the main plantation blocks, while lower heights are associated with recently planted or transitional growth areas.

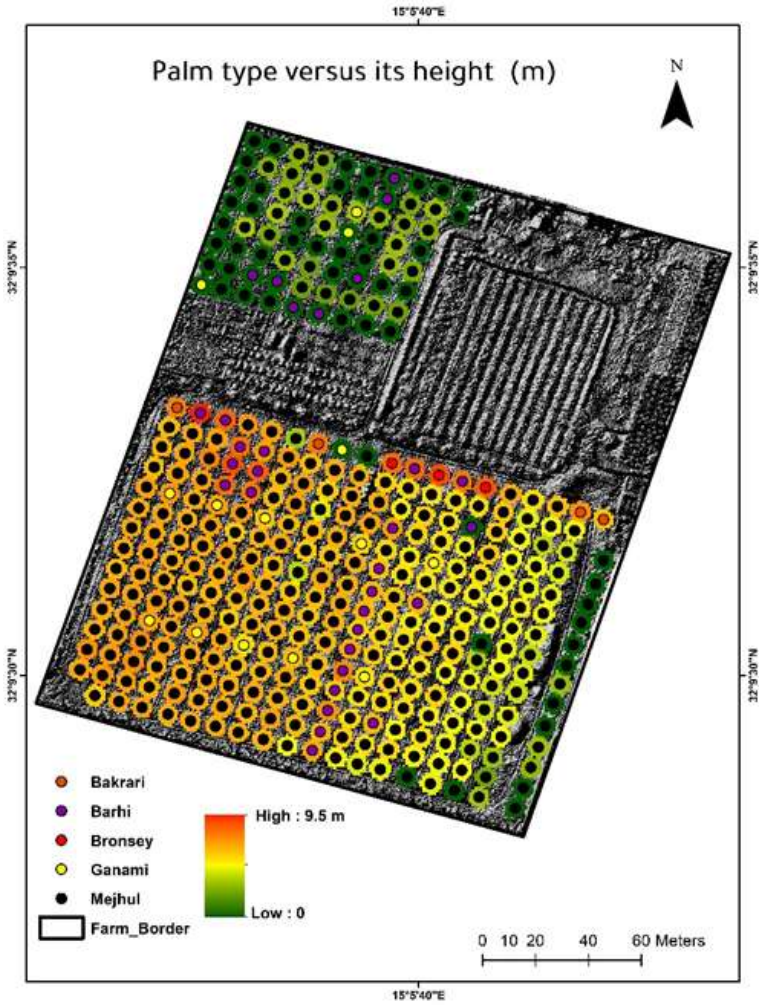

Figure 8. Spatial distribution of palm height (m) derived from photogrammetric elevation data.

The spatial agreement between height and crown diameter distributions confirms structural coherence across development stages. This consistency validates the reliability of the geometric extraction workflow and

demonstrates the capability of UAV-based photogrammetry to capture vertical vegetation structure with sufficient precision for agricultural assessment.

4.3 Spatial Variability and Cluster Analysis

4.3.1 Standard Deviation Analysis

The spatial variability of palm structural attributes was assessed using standardized deviation mapping of both height and crown diameter, as illustrated in Figure 9. The standard deviation classification reveals clear differentiation between zones of homogeneous growth and areas exhibiting structural divergence.

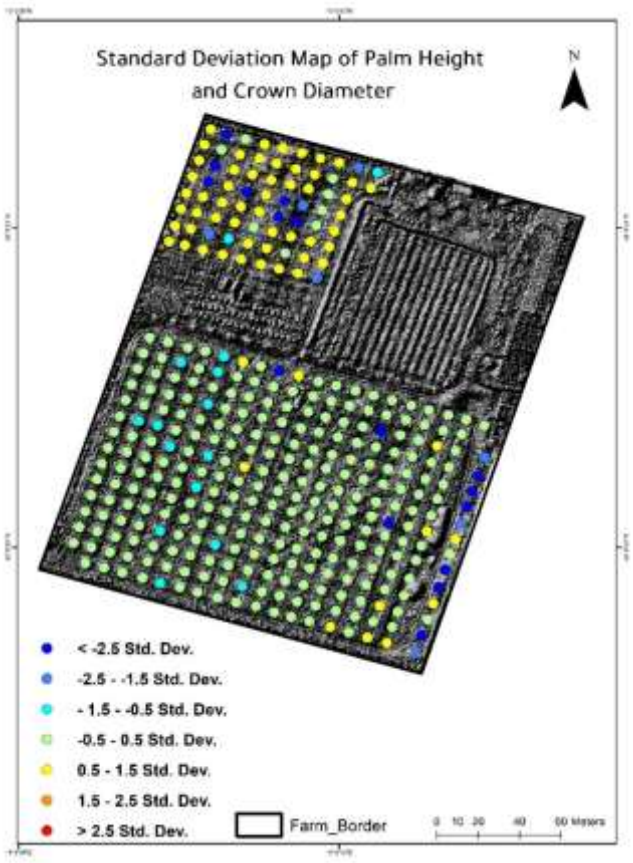

Figure 9. Standard deviation map of palm height and crown diameter

Most mature productive palms fall within the −0.5 to +0.5 standard deviation range, indicating structural uniformity within the main plantation block. In contrast, extreme deviations (> ±2.5 Std. Dev.) are primarily associated with newly planted palms and peripheral zones. These deviations reflect expected biological differences between growth stages rather than measurement inconsistencies.

The concentration of low-variability classes within the primary production area confirms consistent agricultural management practices, including uniform irrigation, spacing, and maintenance regimes.

4.3.2 Spatial Cluster Analysis

To further evaluate spatial organization, a cluster analysis of palm growth attributes (height and crown diameter) was performed, as shown in Figure 10. The results demonstrate strong spatial clustering according to developmental stages.

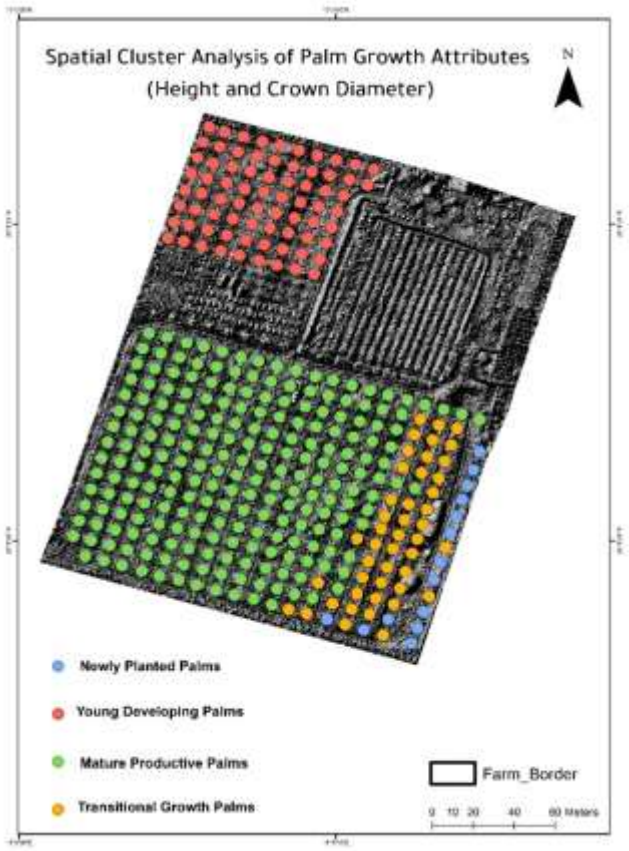

Figure 10. Spatial cluster analysis of palm growth attributes (height and crown diameter).

Four primary growth classes were identified:

- Newly planted palms
- Young developing palms
- Transitional growth palms
- Mature productive palms

The mature productive palms dominate the central and southern plantation blocks, forming strong spatial clusters. Transitional palms are concentrated along the eastern boundary, while newly planted palms are clearly grouped within the northern block.

This structured spatial pattern confirms that palm growth distribution is not random but reflects phased plantation planning. The clustering behavior aligns with the calculated Moran's I value (0.7789), indicating strong positive spatial autocorrelation.

4.4 Density and Distribution Analysis

4.4.1 Kernel Density Estimation

The spatial distribution intensity of palm trees was evaluated using Kernel Density Estimation (KDE), as presented in Figure 11. The density surface highlights the main plantation block as a high-density zone, corresponding to the structured arrangement of mature palms. Lower density values are observed in peripheral and northern areas where palms are either newly planted or sparsely distributed.

The density gradient clearly reflects plantation zoning, with the southern and central sections exhibiting continuous high-density patterns. These results confirm the organized geometric planting structure and demonstrate the effectiveness of KDE in identifying concentration zones and spatial continuity within agricultural landscapes.

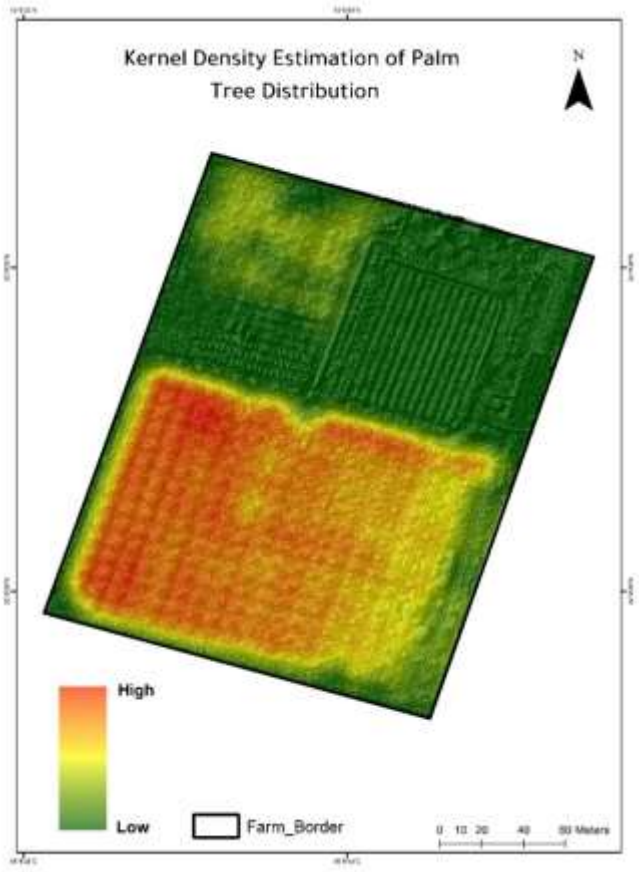

Figure 11. Kernel density estimation of palm tree distribution.

4.4.2 Palm Density Classification

A classified density map was generated to categorize palm distribution into four density classes: None, Low, Medium, and High (Figure 12). The majority of the plantation area falls within the High-density class,

corresponding to the mature production block. Medium-density zones occur in transitional planting areas, while Low-density zones are associated with newly planted sections and infrastructure spaces.

The classification supports quantitative assessment of plantation compactness and allows identification of underutilized or developing areas. Spatial density mapping has been widely applied in geographic and ecological analyses to evaluate distribution intensity and clustering behavior (Silverman, 1986). This spatial differentiation provides a valuable tool for planning expansion, replanting strategies, and yield optimization.

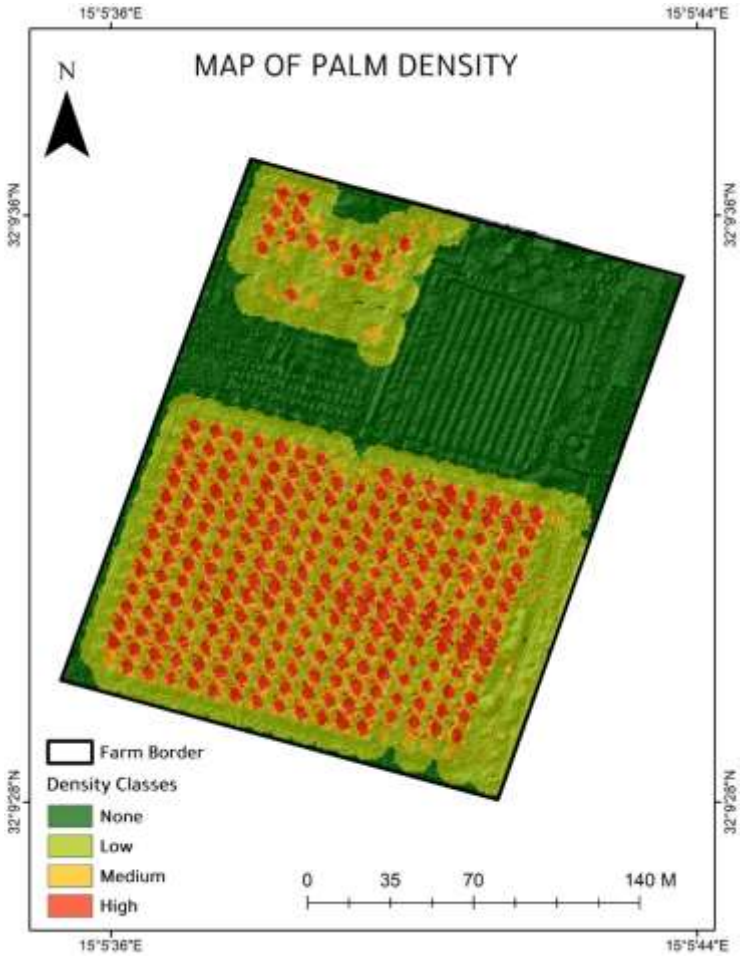

Figure 12. Classified map of palm density within the study area.

4.5 Thermal Analysis

Thermal imagery was integrated with the geometric and spatial datasets to evaluate temperature variation across the plantation. The resulting thermal map is presented in Figure 13. The analysis reveals a clear contrast between vegetated areas and exposed soil surfaces. Mature palm clusters exhibit relatively lower surface temperatures, reflecting active transpiration and canopy cooling effects (Jones, 2004). These areas appear in cooler tonal classes on the thermal map. In contrast, bare soil and sparsely vegetated zones display higher thermal values due to direct solar exposure and reduced evapotranspiration.

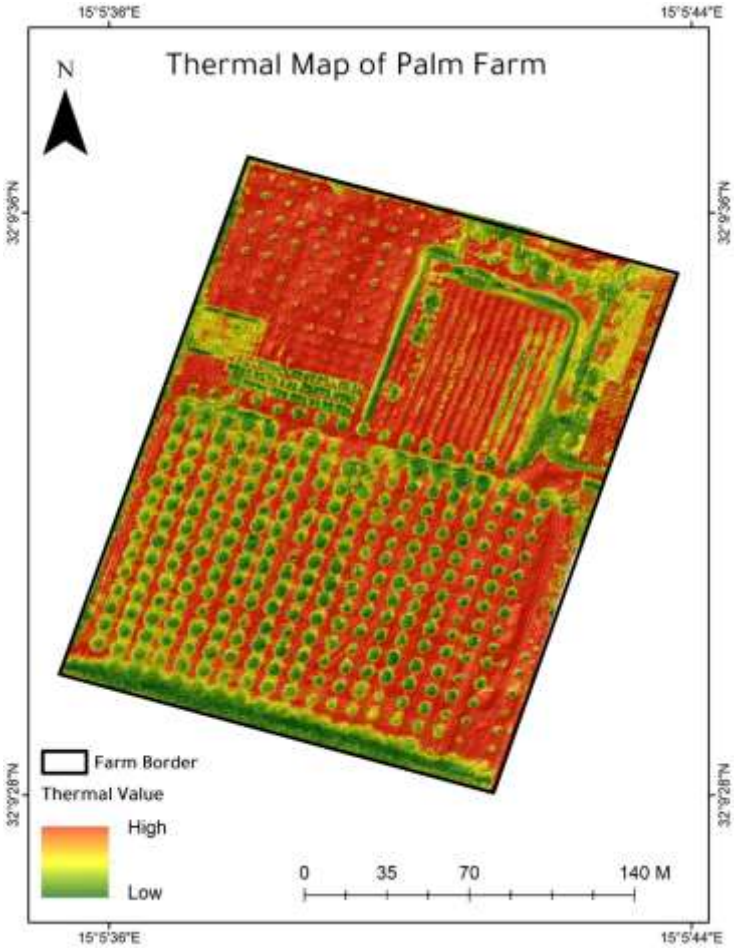

Figure 13. Thermal map of the palm farm derived from UAV-based thermal imagery.

Notably, areas containing newly planted palms correspond to warmer thermal signatures, which aligns with their limited canopy coverage and reduced shading effect. This thermal behavior supports the structural analysis results and further validates the growth-stage classification identified in previous sections. The integration of thermal data enhances the overall assessment by providing insight into plant vigor, water status, and potential stress conditions. The combined geometric and thermal analysis demonstrates the added value of multisensor UAV platforms for comprehensive agricultural monitoring.

4.6 Integrated Geospatial Database and 3D Visualization

All extracted geometric and spatial outputs were integrated into a unified geospatial database within ArcGIS Environment. Each detected palm was assigned a unique Palm_ID linked to its crown diameter, height, and precise spatial coordinates, forming a comprehensive digital inventory of the plantation. This

structured database enables efficient querying, monitoring of growth stages, and spatial analysis of plantation attributes (Longley et al., 2015).

To validate the vertical accuracy and structural consistency of the extracted heights, a Digital Surface Model (DSM) generated from UAV imagery was visualized in the Global Mapper environment, as shown in Figure 14. The three-dimensional representation clearly illustrates canopy elevation differences, with palm crowns appearing as distinct vertical structures above the ground surface. The regular row alignment and height variation between mature and younger palms confirm the reliability of the photogrammetric reconstruction and geometric extraction workflow.

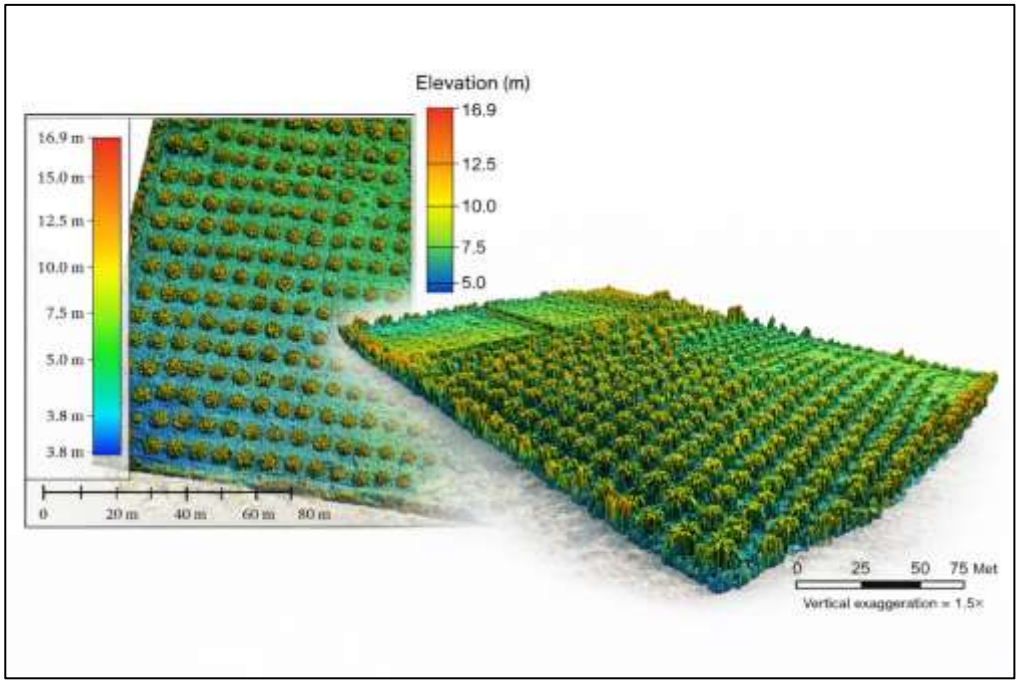

Figure 14. Three-dimensional DSM visualization generated from UAV imagery and displayed in Global Mapper, illustrating palm canopy height variation.

In addition, the functional classification of the farm infrastructure is presented in Figure 15. This map integrates palm distribution with operational components including plantation blocks, storage facilities, gates, water tanks, desalination plant, and auxiliary crop areas. The spatial integration of structural palm data with infrastructure mapping enhances the analytical capability of the system and supports informed decision-making for plantation management and resource allocation.

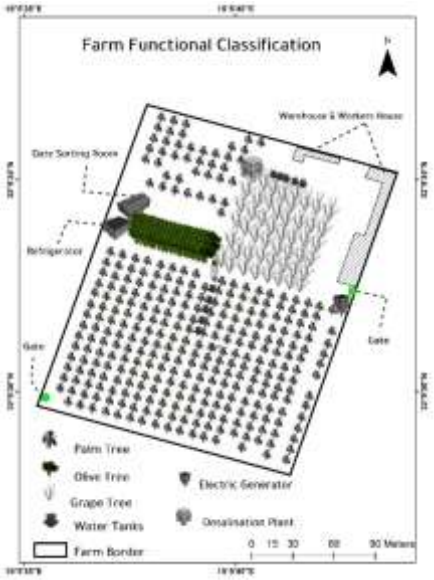

Figure 15. Functional classification map of farm infrastructure and plantation layout.

Furthermore, the spatial classification of date palm varieties is presented in Figure 16. This map illustrates the distribution of Medjool, Barhi, Ghanami (male), Bronzi, and Bakrari palms across the plantation. Each variety is linked to its corresponding Palm_ID within the geospatial database, enabling varietal-level analysis of structural attributes, growth patterns, and spatial clustering. The integration of varietal information with geometric and infrastructural datasets strengthens the analytical depth of the digital plantation model and supports precision management strategies.

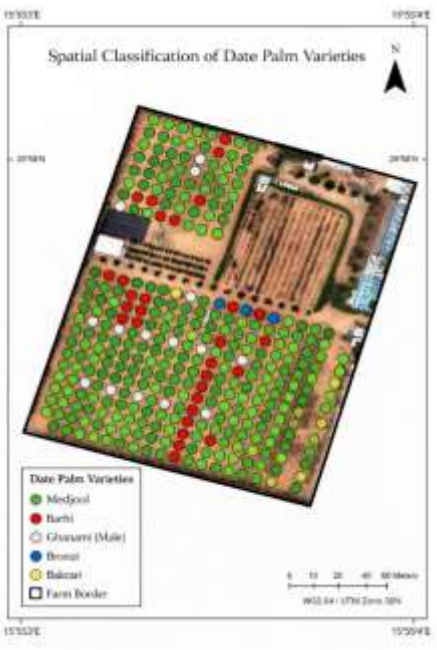

Figure 16. Spatial classification of date palm varieties integrated within the geospatial database framework.

5. Conclusion

This study presented an integrated UAV–AI–GIS framework for automated detection, counting, and structural analysis of date palm trees in a semi-arid agricultural environment. High-resolution UAV imagery (GSD = 1.77 cm/pixel) combined with photogrammetric processing produced geometrically accurate orthomosaic and DSM products (Total RMSE = 5.07 cm), ensuring reliable spatial measurements.

The YOLOv8 deep learning model achieved strong detection performance (mAP@50 = 93.0%, Recall = 95.1%), successfully identifying 310 palms (86% detection rate). Missed detections were primarily associated with very small seedlings, indicating limitations in small-object recognition under low contrast conditions. Morphometric analysis revealed clear spatial differentiation in crown diameter and height, with statistically significant clustering confirmed by Moran's I (0.7789). Thermal analysis supported structural findings by highlighting radiometric contrasts between mature palms and exposed soil areas.

The integration of 2D and 3D DSM visualization further validated vertical structural variability and reinforced the robustness of UAV-derived geometric measurements. The resulting geospatial database provides a scalable digital inventory system capable of supporting precision agriculture, farm management, and long-term monitoring.

6. Future Work

Future research should focus on integrating LiDAR technology with UAV-based photogrammetric data to enhance the accuracy and completeness of three-dimensional surface modeling. The fusion of LiDAR point clouds with photogrammetric DSM and orthomosaic products would improve canopy structure representation, reduce occlusion effects, and increase the precision of height and crown measurements, particularly in dense plantation blocks. Such integration would strengthen vertical accuracy and enable more reliable structural assessment of individual palms.

In addition, future developments may incorporate multispectral sensors combined with thermal imagery to enhance date palm health assessment and stress detection. The integration of spectral vegetation indices (e.g., NDVI and other reflectance-based metrics) with thermal data would improve early identification of water stress, nutrient deficiency, and disease conditions. This multisensor approach would extend the current structural analysis toward comprehensive physiological monitoring, thereby strengthening precision agriculture applications and supporting proactive plantation management strategies.

Acknowledgment

The authors would like to express their sincere appreciation to the Libyan Center for Date Palm Research and Raqeem Information Technology Company for their scientific and logistical support, which was instrumental in the successful implementation of the UAV data acquisition, photogrammetric processing, and analytical phases of this study.

References

1. Ampatzidis, Y. and V. Partel (2019). "UAV-based high throughput phenotyping in citrus utilizing multispectral imaging and artificial intelligence." Remote Sensing **11**(4): 410.

2. Chao, C. T. and R. R. Krueger (2007). "The date palm (Phoenix dactylifera L.): overview of biology, uses, and cultivation." HortScience **42**(5): 1077-1082.

3. El Hadrami, A. and J. M. Al-Khayri (2012). "Socioeconomic and traditional importance of date palm." Emirates Journal of food and Agriculture **24**(5): 371.

4. James, M. R., Robson, S., & Smith, M. W. (2017). 3-D uncertainty-based topographic change detection with structure-from-motion photogrammetry: precision maps for ground control and directly georeferenced surveys. Earth Surface Processes and Landforms, 42(12), 1769-1788.

5. Jones, H. G. (2004). "Application of thermal imaging and infrared sensing in plant physiology and ecophysiology." Advances in Botanical Research 41: 107–163.

6. Laliberte, A. S. and A. Rango (2011). "Image processing and classification procedures for analysis of sub-decimeter imagery acquired with an unmanned aircraft over arid rangelands." GIScience & Remote Sensing **48**(1): 4-23.

7. Li, W., et al. (2016). "Deep learning based oil palm tree detection and counting for high-resolution remote sensing images." Remote Sensing **9**(1): 22.

8. Lin, T.-Y., et al. (2014). "Microsoft COCO: Common objects in context." European Conference on Computer Vision (ECCV): 740–755.

9. Longley, P. A., et al. (2015). Geographic Information Systems and Science. 4th ed. Wiley.

10. Osco, L. P., et al. (2021). "A review on deep learning in UAV remote sensing." International Journal of Applied Earth Observation and Geoinformation **102**: 102456.

11. Rasmussen, J., et al. (2016). "Are vegetation indices derived from consumer-grade cameras mounted on UAVs sufficiently reliable for assessing experimental plots?" European Journal of Agronomy **74**: 75-92.

12. Redmon, J., et al. (2016). You only look once: Unified, real-time object detection. Proceedings of the IEEE conference on computer vision and pattern recognition.

13. Silverman, B. W. (1986). Density Estimation for Statistics and Data Analysis. Chapman & Hall.

14. Torres-Sánchez, J., et al. (2015). "An automatic object-based method for optimal thresholding in UAV images: Application for vegetation detection in herbaceous crops." Computers and Electronics in Agriculture **114**: 43-52.

15. Wallace, L., et al. (2016). "Development of a UAV–LiDAR system with application to forest inventory." Remote Sensing 8(11): 940..

16. Weinstein, B. G., et al. (2019). "Individual tree-crown detection in RGB imagery using semi-supervised deep learning neural networks." Remote Sensing **11**(11): 1309.

17. Westoby, Matthew J., et al. "'Structure-from-Motion'photogrammetry: A low-cost, effective tool for geoscience applications." Geomorphology 179 (2012): 300-314.

18. Zaid, A. (2024). Date palm cultivation, Food & Agriculture Org.[Author][Author].

19. Zaid, A. and E. Arias-Jimenez (2002). "Date palm cultivation FAO plant and protection paper."

20. Zhang, C. and J. M. Kovacs (2012). "The application of small unmanned aerial systems for precision agriculture: a review." Precision agriculture **13**(6): 693-712.